# Description and ecophysiology of a new species of Syndesmis Silliman, 1881 (Rhabdocoela: Umagillidae) from the sea urchin Evechinus chloroticus (Valenciennes, 1846) Mortensen, 1943 in New Zealand

Monnens, Marlies

2019-12

Monnens , M , Frost , E J , Clark , M , Sewell , M A , Vanhove , M P M & Artois , T 2019 , ' Description and ecophysiology of a new species of Syndesmis Silliman, 1881 (Rhabdocoela: Umagillidae) from the sea urchin Evechinus chloroticus (Valenciennes, 1846) Mortensen, 1943 in New Zealand ' , International journal for parasitology. Parasites and wildlife , vol. 10 , pp. 71-82 . https://doi.org/10.1016/j.ijppaw.2019.07.005

http://hdl.handle.net/10138/309027
https://doi.org/10.1016/j.ijppaw.2019.07.005

IJP: Parasites and Wildlife 10 (2019) 71–82

Contents lists available at ScienceDirect

IJP: Parasites and Wildlife

journal homepage: www.elsevier.com/locate/ijppaw

# Description and ecophysiology of a new species of *Syndesmis* Silliman, 1881 (Rhabdocoela: Umagillidae) from the sea urchin *Evechinus chloroticus* (Valenciennes, 1846) Mortensen, 1943 in New Zealand

Marlies Monnens[a,*], Emily J. Frost[b], Miriam Clark[b], Mary A. Sewell[b], Maarten P.M. Vanhove[a,c,d,e], Tom Artois[a]

[a] Hasselt University, Centre for Environmental Sciences, Research Group Zoology: Biodiversity and Toxicology, Agoralaan Gebouw D, B-3590, Diepenbeek, Belgium
[b] School of Biological Sciences, University of Auckland, Private Bag, 92019, Auckland, New Zealand
[c] Department of Botany and Zoology, Faculty of Science, Masaryk University, Kotlářská 2, CZ-611 37, Brno, Czech Republic
[d] Laboratory of Biodiversity and Evolutionary Genomics, University of Leuven, Charles Debériotstraat 32, B-3000, Leuven, Belgium
[e] Zoology Unit, Finnish Museum of Natural History, University of Helsinki, P.O.Box 17, FI-00014, Helsinki, Finland

ARTICLE INFO

*Keywords:*
Flatworm
Systematics
Global warming
Climate change
Echinoidea
Echinodermata

ABSTRACT

A new rhabdocoel of the genus *Syndesmis* Silliman, 1881 (Umagillidae) is described from the intestine of the New Zealand sea urchin *Evechinus chloroticus* (Valenciennes, 1846) Mortensen, 1943a. This new species, *Syndesmis kurakaikina* n. sp., is morphologically distinct and can easily be recognised by its very long ( ± 1 mm) stylet and its bright-red colour. In addition to providing a formal description, we present some observations on reproduction and life history of this new species. Fecundity is comparable to that of other umagillids and the rate of egg production and development increases with temperature. Hatching in this species is induced by intestinal fluids of its host. Relevant to global warming, we assessed the effect of temperature on survival, fecundity, and development. The tests indicate that *Syndesmis kurakaikina* n. sp. is tolerant of a wide range of temperatures (11–25 °C) and that its temperature optimum lies between 18.0 and 21.5 °C. Egg viability is, however, significantly compromised at the higher end of this temperature range, with expelled egg capsules often being deformed and showing increasingly lower rates of hatching. Given this, a rise in global temperature might increase the risk of *Syndesmis kurakaikina* n. sp. infecting new hosts and would possibly facilitate the spread of these endosymbionts.

## 1. Introduction

*Evechinus chloroticus* (Valenciennes, 1846) Mortensen, 1943a, known generally by its Māori name 'kina', is an echinometrid sea urchin endemic to coasts of New Zealand. It has a broad geographical distribution around the main islands of New Zealand and is most commonly found in shallow, moderately exposed waters (Barker, 2013). As an important grazer of kelp and other macroalgae, this echinoid plays a keystone role in local ecological communities (Villouta et al., 2001). *Evechinus chloroticus* also has considerable economic and cultural value, as these urchins are commercially harvested to supply 'roe' (the edible gonads) to (mainly) domestic markets, and kina are an important component of local customary and recreational fisheries (Miller and Abraham, 2011). As echinoderms are particularly vulnerable to external stressors, especially in the early life stages (Przeslawski et al., 2015), much research has been conducted to estimate their response to current and near-future anthropogenic climate change (e.g., Wood et al., 2008; Byrne et al., 2009; Dupont et al., 2010). For the specific case of *E. chloroticus*, ocean acidification, temperature increases, and fluctuations in salinity around New Zealand will likely have severe impacts on kina populations (Clark et al., 2009; Delorme and Sewell, 2013, 2016).

A factor yet to be considered in this scenario is the effect of climate change on the (endo)symbiont communities associated with *E. chloroticus*. In other taxa, increased temperatures have been found to be positively correlated with infectivity as well as with the production and emergence of free-swimming life stages of parasites (e.g., Poulin, 2005; Macnab and Barber, 2011). However, life-history traits of parasites not only vary with different abiotic conditions but are also dependent on changes in the host environment (see review by Altizer et al., 2013). On

* Corresponding author.
*E-mail addresses:* marlies.monnens@uhasselt.be (M. Monnens), efro833@aucklanduni.ac.nz (E.J. Frost), clarkrmb@gmail.com (M. Clark), m.sewell@auckland.ac.nz (M.A. Sewell), maarten.vanhove@uhasselt.be (M.P.M. Vanhove), tom.artois@uhasselt.be (T. Artois).

https://doi.org/10.1016/j.ijppaw.2019.07.005
Received 30 April 2019; Received in revised form 9 July 2019; Accepted 10 July 2019

the other hand, parasite diversity may be negatively affected by climate change, with projections predicting extinction of substantial proportions of parasite species (Carlson et al., 2017). Making generalised predictions on the effects of a changing climate on parasitism, therefore, remains a complex challenge and different species can be expected to show different ecological responses (Marcogliese, 2001).

Studies addressing the parasite and/or (endo)symbiont communities of *E. chloroticus* are limited: McRae (1959) observed several bright-red flatworms (Platyhelminthes Minot, 1876) in the urchin's intestine. He considered these flatworms to represent a new species of *Syndesmis* Silliman, 1881 (Umagillidae, Rhabdocoela) but provided only a very brief characterisation. What is presumed to be the same species was later reported from the same host by Dix (1970) and, more recently, James (2007) also reported an infection of *Syndesmis* sp. in the gut of *E. chloroticus*. However, a detailed taxonomic account of this umagillid is still lacking and, to our knowledge, no preserved material of this species exists.

In this study, a new species of *Syndesmis* is described that was found infesting *E. chloroticus* in large numbers. Light microscopy, differential-interference contrast (DIC), and scanning electron microscopy (SEM) were used to study its morphology. In addition, the different life stages of this species were investigated in detail through a range of *in vitro* experiments to assess the effect of increasing sea-water temperatures on the life-history traits of this flatworm.

## 2. Materials and methods

### 2.1. Sampling of endosymbionts

Adult specimens of *E. chloroticus* were collected from dense aggregations of sea urchins at 2–4 m depth by free-diving at Matheson's Bay (36°18′10″S, 174°47′57″E) or Omaha Cove (36°17′30″S, 174°48′33″E), on the north-east coast of New Zealand. Sea urchins were transported to the city campus of the University of Auckland and kept in aerated tanks (30 urchins per 80L tank) of UV-irradiated, autoclaved and filtered (1 μm mesh) seawater (AFSW); 50–100% of the seawater was changed every 2–3 days. Urchins were kept under constant environmental conditions (18.0 °C; 12:12 light:dark cycle) and fed every three days to satiation with fresh kelp [*Ecklonia radiata* (Agardh, 1817) Agardh 1848]. Urchins were taken from this tank within one week of collection for extraction of flatworms. Sea urchins that were later used to provide intestinal fluids for hatching experiments were transferred to aerated seawater buckets (one 10L bucket per 5–6 urchins; all environmental and feeding conditions as described above). No ethical approval was required for collection or maintenance of the sea urchins under New Zealand law.

Live endosymbionts were collected from the intestinal compartment of *E. chloroticus* by cutting the aboral half of the sea urchin test using scissors (Fig. 1A). Live flatworms (Fig. 1B and C) were flushed from the intestines using plastic transfer pipettes and placed in 24-ml glass scintillation vials filled with AFSW for preservation or incubation experiments as described below.

### 2.2. Morphological characterisation and species description

To examine the general morphology of collected flatworms, specimens were fixed in 4% formalin and subsequently transferred to a 70% EtOH solution. Specimens intended for whole-mounts were then cleared and preserved in lactophenol on glass microscope slides. Study of non-sclerotised morphological structures used 4-μm serial sections prepared from paraffin blocks cut in sagittal, frontal, and transverse orientations. Sectioned specimens were stained with Haidenhein's haematoxylin and eosin as counterstain.

Prepared slides were photographed using a Leica DM2500 LED microscope equipped with the Leica Application Suite X (LAS X) software. DIC was used for whole-mounts and standard light microscopy settings for histological sections. As the position of the sclerotised part of the copulatory organ could not be captured in a single photograph, we compiled a single, projecting image from 36 photographs together Adobe Photoshop CS5.1. Scaled drawings of internal structures were produced using a camera lucida, scanned, and traced using the pen tool in Adobe Illustrator CS5.1. Positions of internal structures are expressed as a percentage of total body length (distance from the anterior tip of the body). Measurements were taken along the central axis of each structure.

Intact and broken (hatched) egg capsules from *Syndesmis* were obtained from temperature-incubation experiments, as described below, during the late winter. Egg capsules were fixed for 1 h in 2.5% glutaraldehyde in phosphate buffer (0.1 M phosphate, 0.14 M sodium chloride, pH 7.4), rinsed in phosphate buffer for 15 min, and post-fixed for 1 h in 2% osmium tetroxide in the same phosphate buffer. Following the second fixation, capsules were rinsed twice for 10 min in phosphate buffer, dehydrated in an ascending series of ethanol (30%, 50% and 70% EtOH, 15 min each), and stored in 70% ethanol for 36 h before continuing the dehydration process through the ethanol series (90%, 95%, and two changes of 100%, 15 min each). Capsules were critical-point dried with 99.99% $CO_2$, coated with platinum (20 nm), and examined with a Quanta 200 FEG ESEM scanning electron microscope.

The holotype specimen has been deposited in the natural sciences collection of the Auckland museum in New Zealand (AIM MA73591). Paratypes were also deposited here (AIM MA73592-MA73595), as well as in the collections of the research group 'Zoology: Biodiversity and Toxicology' of Hasselt University (UH 725-737) and in the zoological collections of the Finnish Museum of Natural History (MZH KV623-632). Species authorships are by Monnens, Vanhove & Artois (International Commission on Zoological Nomenclature, 2015).

### 2.3. Reproductive characteristics

Endosymbionts were experimentally manipulated to obtain egg capsules and to provide preliminary information on the length of development and time to hatching. We exposed individuals to five biologically relevant temperatures from 11.0 to 25.0 °C. This covers the temperature range that *E. chloroticus* is currently exposed to in its natural environment in Northern New Zealand (13–23 °C, Shears and Bowen, 2017) plus and minus 2 °C. These temperatures were chosen to represent temperatures experienced by urchin populations located slightly further south (11.0 °C) and the expected summer temperature urchins will be subjected to due to ocean warming by the year 2090 (25 °C, IPCC, 2014). Experiments were repeated in autumn (April), early winter (June), late winter (August), and spring (October) when local sea surface temperatures were 20.5, 16.0, 14.5, and 15.0 °C, respectively.

Preliminary experiments identified AFSW as a suitable medium for short-term incubation of the flatworms, provided the sea urchin intestinal fluids were removed by first rinsing the worms in AFSW (Clark, 2017, unpublished Honours Dissertation). Four clean, adult worms were placed into 25 fully filled 24-ml glass scintillation vials of AFSW and cultured for four days in an aluminium temperature block with a gradient of temperatures between the cold (5.0 °C) and hot (30.0 °C) water baths at opposite ends. Flatworms were incubated at five different temperatures (11.0, 14.5, 18.0, 21.5, and 25.0 °C), with five biological replicates: four worms in each replicate, taken from the same urchin specimen, and one control (AFSW filled vials without worms) that was used to monitor the temperature throughout the course of the study using a digital thermometer (Jenway 3510 pH Meter).

A pilot study confirmed a high rate of survival (82%) for flatworms maintained in seawater for the first four days, subsequent to which the animals started to senesce. Every 24 h for the 4-day incubation, each vial was checked for flatworm survival, with animals identified as dead through lack of attachment and loss of their bright-red colour. After four days, adult worms were removed from the 24-ml scintillation vials

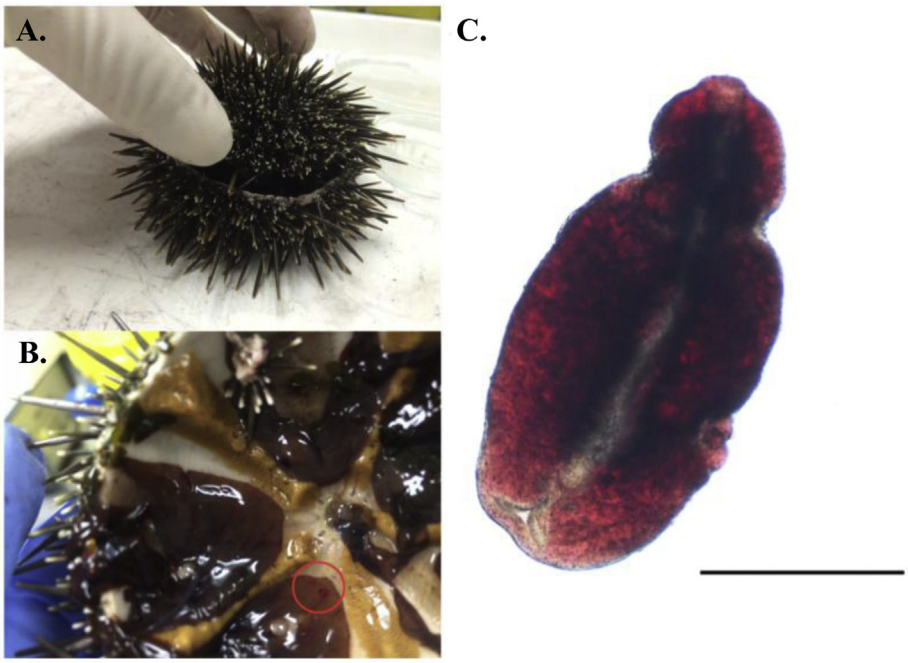


**Fig. 1. A.** Specimen of *E. chloroticus* showing the horizontal plane of dissection. **B.** Urchin intestines containing flatworms (circled). **C.** Live specimen of *Syndesmis kurakaikina* n. sp., showing its bright-red colour. Scale bar: 1 mm. (For interpretation of the references to colour in this figure legend, the reader is referred to the Web version of this article.)

and the seawater was transferred into a Petri dish, where the number of egg capsules (fecundity) was counted using a dissecting microscope at 6x magnification. After counting, the AFSW in each vial was replaced and the vials were returned to the temperature block for long-term monitoring of capsule development. Each week, the stage of embryo development was determined by transferring isolated capsules onto depression slides and photographing them on a Nikon Ti-E inverted microscope at 400x magnification using the NIS-Elements AR 3.2 64-bit Imaging Software (standard and real-time EDF photos).

Hatching success in the different temperatures was tested in a 1:1 mixture of sea urchin intestinal fluid and AFSW. Intestinal fluid was obtained from dissected sea urchins by cutting the anterior part of the intestines and squeezing out the contents into a glass Petri dish using forceps. Due to the small quantity of intestinal fluid that could be obtained, hatching trials were conducted in plastic 96-well tissue-culture plates placed on top of the incubation block at 16.5, 18.0, 20.0, 22.0, and 24.5 °C. Capsules were first tested after ca. two weeks, when a subset of the embryos was first observed moving in the capsules, by incubating the capsules in intestinal-fluid-AFSW for four days. Hatched capsules were counted and photographed. Unhatched capsules were returned to the source vial with AFSW and incubated for a further two weeks. The hatching test was then repeated at approximately four weeks post-laying in the intestinal fluid-AFSW solution.

Using RStudio v0.98.1103 (R Development Core Team, 2017), a Linear Mixed Model (LMM) was used to analyse the number of egg capsules laid in the different temperature treatments during the four different seasons. The data were log-transformed to satisfy the underlying assumption of homoscedasticity required by the LMM. The model also included a random effect term to allow for correlations between multiple measurements (endosymbionts) from each urchin. Note that while a Generalised Linear Mixed Model would have been preferred for this low-value count data, this model would not converge and hence the log-transformed LMM was used as the best alternative. Pairwise comparisons of means were made between temperatures within seasons and between seasons within temperatures, using Tukey's Honestly Significant Difference tests to adjust for multiple comparisons. The $\alpha = 0.05$ level of significance was used.

## 3. Results

### 3.1. Taxonomic account

*Syndesmis kurakaikina* n. sp. Monnens, Vanhove and Artois.

**Type locality**. Matheson's Bay (36°18′10″S, 174°47′57″E), on the north-east coast of New Zealand.

**Type host**. *Evechinus chloroticus* (Echinometridae, Echinoidea).

**Type material**. Twenty whole-mounts made permanent with lactophenol, one of which was designated the holotype (AIM MA73591), the rest paratypes (AIM MA73592; UH 725-732; MZH KV623-628). Six sagittally sectioned, four frontally sectioned, and three transversely sectioned specimens, all of which were designated paratypes (AIM MA73593-73595; UH 733-737; MZH KV629-632).

**Etymology**. The species epithet refers to the Māori terminology for 'bright red' (kura), 'to eat' (kai) and the type host, *E. chloroticus* (kina).

**Occurrence in host**. Typically at low infection intensity of ~10 specimens per sea urchin. However, the number of flatworms observed in the intestines of urchins from northern New Zealand in the summer of 2016 was unusually high, with counts ranging from 29 to 368 and an average of 165 (n = 72).

**Notes on terminology**. The terminology pertaining to the different components of the (female) reproductive system in representatives of *Syndesmis* has become confusing. For instance, the term 'female antrum' (or 'antrum feminum') has been used inconsistently, as it sometimes refers to the distal end of the uterus (e.g., Smith, 1973), and sometimes to the (often-expanded) posterior end of the vagina (e.g., Moens et al., 1994). Furthermore, different terms have often been used to describe the same structures. For example, the duct connecting the distal end of the uterus to the ovaries and vitellaria has been called the 'female duct' (e.g., Moens et al., 1994), 'ovovitelline duct' (e.g., Hertel et al., 1990), and 'ductus communis' (e.g., Hickman, 1956). We suggest employing the terminology applied in the caption to Fig. 2.

**Description.** Living specimens have a bright-red colour and can occur at high infection intensities in the intestines of sea urchins. The body is flattened dorsoventrally. The anterior and posterior body ends are rounded (Fig. 3). Body length varies between 1.7 and 2.6 mm ($\bar{X}$ = 2.3 mm, s = 0.37 mm, n = 20) and the body is between 0.7 and 1.5 mm broad ($\bar{X}$ = 1.1 mm, s = 0.18 mm, n = 20) (measured on fixed, whole-mounted specimens).

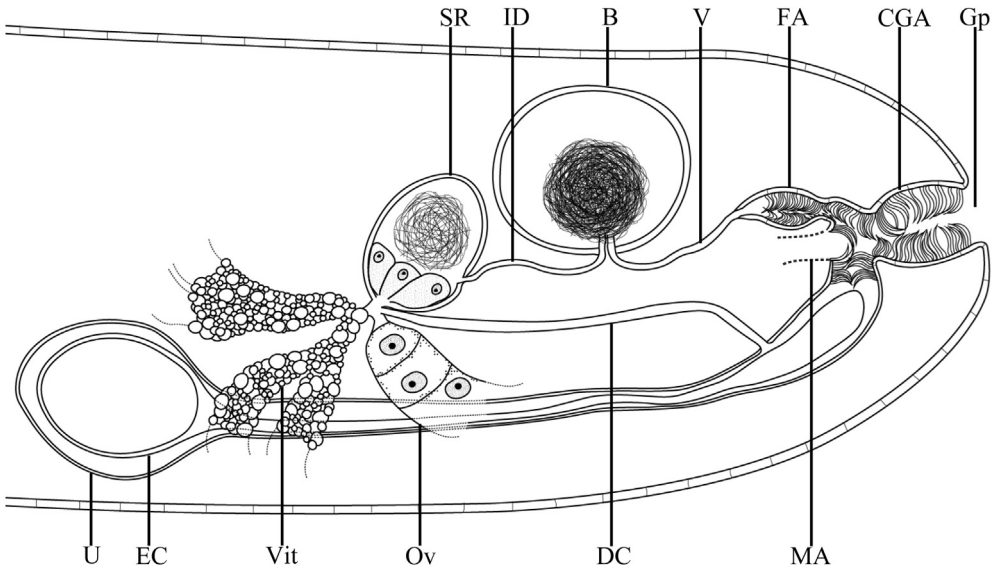


**Fig. 2.** Schematic overview of the female reproductive system in *Syndesmis*. B: bursa, CGA: common genital atrium, EC: egg capsule, FA: female atrium, ID: insemination duct, MA: (entrance to) male atrium, Ov: ovary, Ph: pharynx, St: stylet, SR: seminal receptacle, U: uterus, V: vagina, Vit: vitellaria.

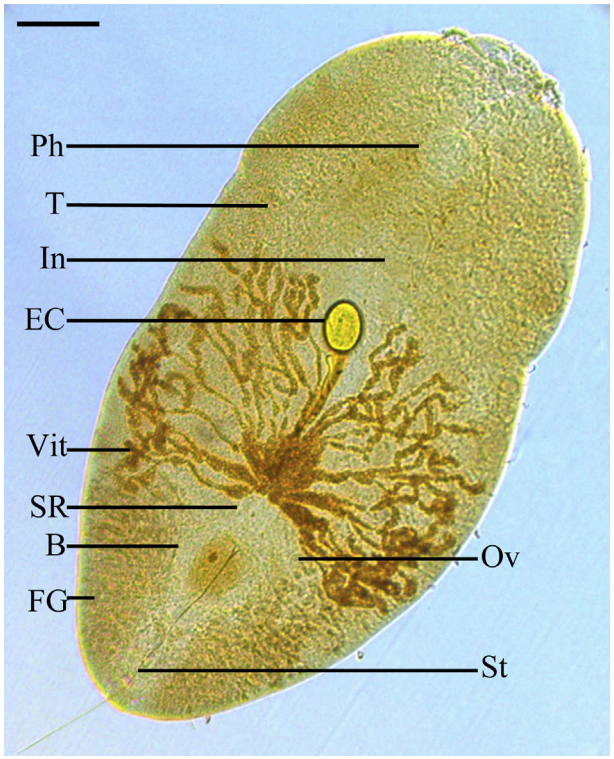


**Fig. 3.** *Syndesmis kurakaikina* n. sp., holotype specimen whole-mounted in lactophenol. Differential-interference contrast. Scale bar: 250 µm. B: bursa, EC: egg capsule, FG: filament glands, In: intestine, Ov: ovaria, Ph: pharynx, St: stylet, SR: seminal receptacle, Vit: vitellaria.


**Fig. 4.** *Syndesmis kurakaikina* n. sp., ciliated invagination at the anterior end in sagittal section. Scale bar: 50 µm. Br: brain.

The epidermal epithelium is non-syncytial. Each epidermal cell is anchored to a thin, folded basement membrane. Epithelial nuclei appear round or oval, with a diameter of approximately 3.5 µm, and occur in the centre or near the basal end of the cells. Epithelial cells vary in shape and thickness across the body. Generally, the ventral epithelium is more flattened, the smallest cells being only 2–3 µm thick. Dorsally, epithelial cells tend to be more or less columnar to cuboidal in shape near the caudal and rostral ends, reaching lengths up to 15 µm. In between these areas, the dorsal epidermal cells are more similar in shape and size to the ventral epidermal cells. The ventral epidermis is completely ciliated except for on the posterior 1/10 of the body. The dorsal epidermis, in contrast, is devoid of cilia, with the exception of on the first 1/10 of the body. Near the anterior end, the epidermis shows a pronounced ventral invagination (Fig. 4). Within this invagination, epidermal cells are columnar in shape and comparatively tall, measuring approximately 20 µm and carrying long cilia (up to 15 µm).

Under the basement membrane, two distinct layers of body wall musculature are visible: an outer circular layer and an inner longitudinal layer. Several bundles of muscle fibres pass dorsoventrally through the body. These fibres are attached to the epidermal basement membrane or to internal organs (mainly the intestine and the pharynx). Space between organs is filled by large parenchyma cells.

The brain is situated immediately rostral to the pharynx. Eyes are lacking. The mouth is positioned subterminally and it opens directly into the buccal cavity. This cavity is a simple, small infold of the ventral epidermis. Epithelial cells in this region are thin and some flattened nuclei are visible here. No buccal glands were observed. The buccal

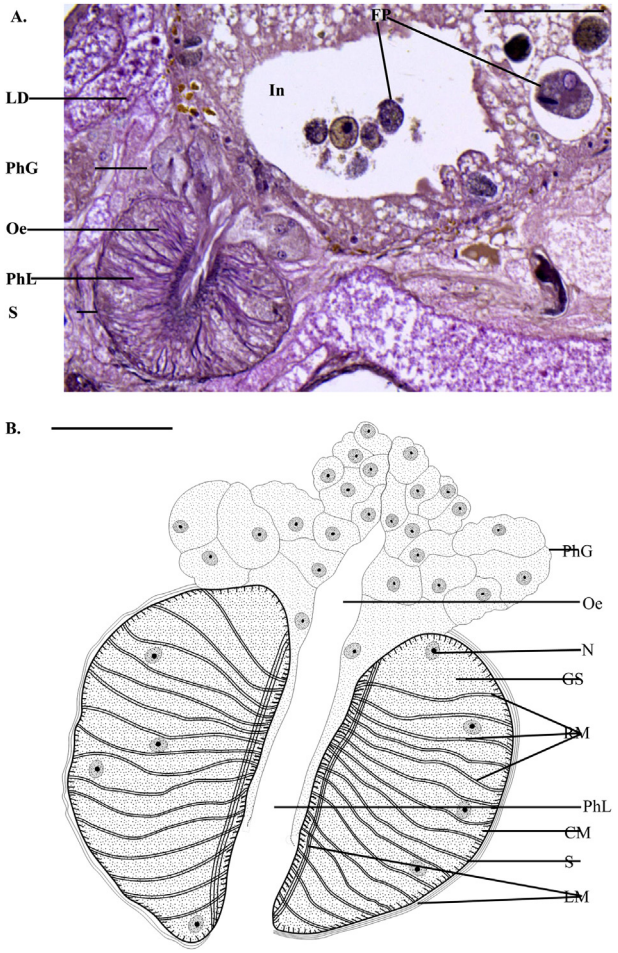


**Fig. 5.** *Syndesmis kurakaikina* n. sp. **A.** Sagittal section through pharynx and intestine. **B.** Camera-lucida drawing of the pharynx and associated glands. Scale bars: A = 100 µm, B = 50 µm. CM: circular muscles, FP: food particles, GS: granular secretion, In: intestine, LD: lipid droplets, LM: longitudinal muscles, N: nucleus, Oe: oesophagus, PhG: pharyngeal glands, PhL: pharyngeal lumen, RM: radial muscles, S: septum.

cavity is connected to the narrow pharyngeal lumen (Fig. 5: PhL). The pharynx is of the doliiform type and measures between 122 and 185 µm in diameter ($\bar{X}$ = 147 µm, s = 19.0 µm, n = 20) (Fig. 5). A pronounced septum separates the pharynx from the surrounding parenchymal tissue (Fig. 5: S). The pharynx is surrounded by an outer longitudinal muscle layer (Fig. 5B: LM) and, immediately at the inside of the septum, a circular one (Fig. 5B: CM). Several thin radial muscles connect the basement membrane of the pharyngeal epithelium surrounding the lumen to the septum (Fig. 5B: RM). Small, round nuclei occur in between these muscles (Fig. 5: N), most of them near to the septum. We hypothesise that these nuclei might be associated with intrapharyngeal glands, though these were not clearly visible in any of our specimens. The pharynx is filled with granular secretion (Fig. 5B: GS). The epithelium of the pharyngeal lumen is surrounded by an outer longitudinal and an inner circular muscle layer (Fig. 5B: LM and CM). Both of these layers consist of numerous, parallel-running muscle fibres. The longitudinal muscles run parallel to the pharyngeal lumen and continue under the epithelium of the oesophagus (Fig. 5: Oe).

Several fragments of dark-staining muscle fibres are visible around the pharynx. Though we could not trace these in their entirety, they seem to attach the pharynx to the epidermis. The pharynx is connected to the intestine through a short oesophagus (34–40 µm, $\bar{X}$ = 35 µm, s = 4.1 µm, n = 6) (Fig. 5A and B: Oe), lined by a thin epithelium and a thin layer of longitudinal muscles. Adjacent to the oesophagus lie two groups of pharyngeal glands (Fig. 5A and B: PhG). Each gland consists of several large, faintly granular cells, each one containing a single round nucleus. These glands line the pharyngeal lumen and seem to empty near the buccal cavity, though this is difficult to observe (Fig. 5B).

The intestine (Figs. 5A, 6 and 7: In) is a large, lobulated blind sac, extending from the caudal end of the oesophagus to the bursa. It is positioned mediodorsally, measures approximately 3/4 of the total body length ( ± 1.2 mm), and has a diameter of ± 160 µm. Posteriorly, the intestine tapers toward a narrow end, which extends dorsally to the seminal receptacle (Fig. 7). The spacious intestinal lumen is lined by tall columnar cells and contains numerous food particles at different stages of digestion (Fig. 5: FP). Intestinal cell boundaries are indistinct and the cells contain numerous vacuoles, some of which also contain one or two relatively large (diameter up to 27 µm) food particles (Fig. 5: FP). Nuclei are usually located near the outer surface of the intestine. Here, cell boundaries are especially difficult to observe. Scattered throughout the intestinal epithelium are several small, orange coloured lipid droplets.

The middle third of the body is largely occupied by two conspicuous vitellaria (Figs. 3, 6 and 7: Vit). Both glands are filled with large amber coloured vitelline droplets. Each vitelline gland consists of four to five main branches, extending forward and laterally and dividing dichotomously to form numerous ultimate branches. Positioned just behind

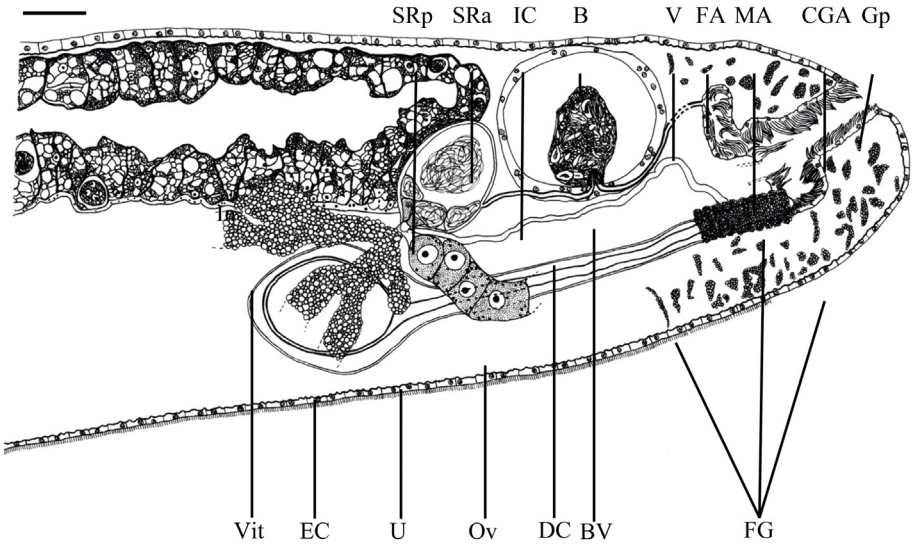


**Fig. 6.** *Syndesmis kurakaikina* n. sp., reconstruction of the female reproductive system from a sagittally sectioned specimen. Male reproductive system omitted. Scale bar: 100 µm. B: bursa, BC: bursal canal (simplified), BV: bursal valve, CGA: common genital atrium, DC: ductus communis, EC: egg capsule, IC: insemination canal, In: intestine, FA: female atrium, FG: filament glands, Gp: gonopore, MA: (entrance to) male atrium, Ov: ovary, SRa: anterior part of seminal receptacle, SRp: posterior part of seminal receptacle, U: uterus, Vit: vitellaria.


**Fig. 7.** *Syndesmis kurakaikina* n. sp., sagittal section through parts of the female reproductive system. Scale bar: 50 µm. B: bursa, DC: (entrance to) ductus communis, In: intestine, Ov: ovary, SRa: anterior part of seminal receptacle, SRp: posterior part of seminal receptacle, Vit: vitellaria.

the vitellaria are two lobulated ovaries (Figs. 3, 6 and 7: Ov), each consisting of one main trunk, which extends laterally a short distance and divides into three short lobes.

The seminal receptacle is lined by a thin epithelium and consists of an anterior and a posterior region (Figs. 6 and 7: SRa and SRp). The former is oriented anteroventrally and is composed of several smaller compartments filled with sperm. Here, multiple large, granular secretory cells occur (Fig. 6: SRa). The posterior region is almost spherical and is also filled with sperm cells (Figs. 6 and 7: SRp). No musculature was observed around the seminal receptacle. A short, sclerotised insemination canal (4–5 µm in diameter; $\bar{X}$ = 4 µm, s = 0.3 µm, n = 5) connects the posterior end of the seminal receptacle to the ventral side of bursa (Fig. 6: IC), where it ends in a sclerotised bursal valve (Fig. 6: BV). The valve measures ± 25 µm in height and projects into the bursal cavity. The bursa appears as a large slightly lobed structure in the hind end of the body (Figs. 6–8: B). It is positioned posteriorly to the seminal receptacle (Fig. 6). In all observed specimens, the bursa contains a dense mass of partially digested sperm cells (Fig. 6). Numerous small nuclei are scattered throughout the thick bursal tissue. From the bursal valve, another sclerotised canal originates: the vagina (Figs. 6 and 8: V). From whole-mounted specimens, it is clear that this duct is very long

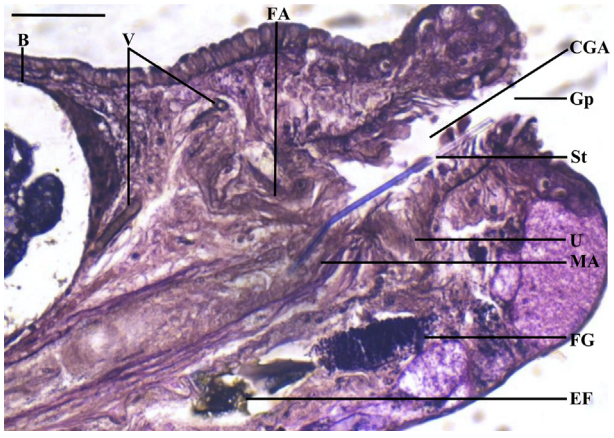


**Fig. 8.** *Syndesmis kurakaikina* n. sp., sagittal section through posterior body end, at genital pore. Scale bar: 50 µm. B: bursa, EF: egg filament, FA: female atrium, FG: filament glands, CGA: common genital atrium, Gp: gonopore, MA: male atrium, St: stylet, U: uterus, V: vagina.

and tightly coiled onto itself. However, as is often the case for sclerotised structures, it consistently shattered during sectioning, making it impossible for us to trace it in its entirety. Distally, the vagina connects to the female atrium (Figs. 6 and 8: FA). The latter is a simple ovoid cavity, lined with high, folded epithelium, giving the appearance of cilia. It enters the common genital atrium on the dorsal side (Figs. 6 and 8: CGA).

Vitellaria, ovaries, and bursa all empty into a narrow, non-muscular ductus communis (Figs. 6 and 7: DC). The last connects these three organs to the uterus (Fig. 6). Generally, this duct is only faintly visible and it could only be completely traced and measured in a single specimen. In that specimen, the ductus communis is ± 370 µm long.

The uterus is situated medioventrally (Figs. 6 and 8: U). The anterior end is expanded and can contain an amber coloured egg capsule (Figs. 3 and 6: EC). This capsule is usually situated in the first body half (as in Fig. 3) but in some specimens, it lies more to the caudal end of the body. Egg capsules are 139–168 µm long ($\bar{X}$ = 152 µm, s = 11.5 µm, n = 19) and 108–148 µm ($\bar{X}$ = 123 µm, s = 10.9 µm, n = 19) broad. SEM revealed that egg capsule bulbs are completely smooth, lacking any structural pattern (Fig. 9A–C). Egg capsule shells are approximately 3 µm thick (Fig. 9G). Each capsule has a long, usually tightly coiled filament ( ± 7 mm), with a woven, porous structure in anterior parts (Fig. 9D) and a smoother surface overlaid with ridges in posterior parts (Fig. 9E). In a small number of specimens, the filament is considerably shorter and/or uncoiled. The egg filament's distal end is slightly expanded. Filament glands are numerous and occupy the major part of the last body third (Figs. 6 and 8: FG). They all empty separately into the distal end of the uterus. The uterus connects to the common genital atrium on its ventral side (Fig. 8).

Two elongate, follicular testes are positioned ventrolaterally, extending from the hind end of the pharynx to approximately 2/3 of the body length (Fig. 10: T). They consist of multiple lobes and are filled with sperm cells at different stages of development. Mature sperm cells occur throughout the whole testis but are most commonly found in the middle region. From here, two wide sperm ducts, filled with mature sperm cells, depart (Fig. 10: SD). Conspicuous glandular tissue surrounds the base of these ducts. The ducts briefly coil dorsally before uniting with one another, after which the resulting duct runs laterally before bending sharply towards the anterior body end. From his point onwards, it rapidly becomes narrower, its diameter decreasing gradually from approximately 50 µm proximally to a mere 10 µm more distally. At about 25% of the body length, the duct bends sharply backwards and subsequently unites with the sperm duct from the opposing testis, before entering the seminal vesicle (Fig. 10: SV). The latter is a slender structure filled with sperm cells and surrounded by well-developed outer circular and inner longitudinal muscle layers. Its diameter gradually decreases distally, continuing as the ejaculatory duct (Fig. 10: ED).

The ejaculatory duct is a long canal filled with sperm (Fig. 10: ED). It is lined with a high epithelium and an inner longitudinal and an outer circular muscle layer. Distally, this duct empties into a long sclerotised stylet (Figs. 8, 10 and 11: St). The stylet is a slender tube which stains light blue with haematoxylin (Fig. 8: St). The proximal end is funnel shaped (Fig. 11) and it is positioned in the second body half, at approximately 2/3 to 3/4 of the total body length. Distally, the stylet terminates in an open, slightly flared tip. The stylet measures between 845 and 1121 µm ($\bar{X}$ = 984 µm, s = 98.7 µm, n = 18) in length, about 40–50% of the total body length. It is enclosed in the male atrium, from where it can protrude into the common genital atrium, and (at least in compressed specimens) outside the body through the gonopore (as in Fig. 3). In most whole-mounts, the stylet is coiled inside the body and describes one or two sharp bends or loops (as in Fig. 11).

The male atrium is an elongate narrow duct, lined by a folded epithelium (Figs. 8 and 10: MA). Both the atrium as well as the ejaculatory duct and the seminal vesicle are lined by a thin continuous sheath (Fig. 10). Just before the base of the stylet the epithelium folds

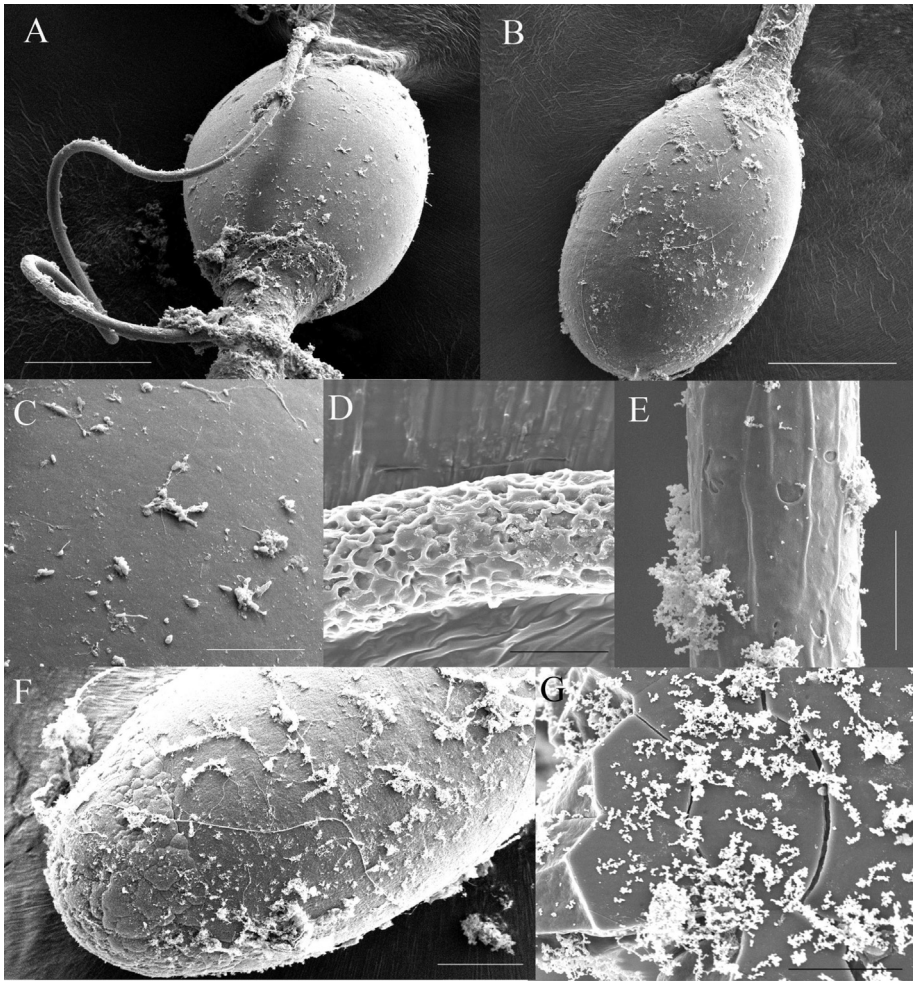


**Fig. 9.** Egg capsules of *Syndesmis kurakaikina* n. sp. **A.** Entire capsule bulb overlaid by part of the long filament. **B.** An egg capsule bulb in its entirety. **C.** Surface of capsule. **D.** Anterior and **E.** posterior parts of the egg filament. **F.** Anterior side of an egg capsule with hatching sutures just prior to opening. **G.** Broken capsule shell. Scale bars: A-B = 50 µm, C = 10 µm, D-E = 5 µm, F = 20 µm.

back onto itself, where it attaches to the stylet. This folded part of the epithelium is comparatively tall. Several indistinct thin muscle fibres are present in this area. Although difficult to differentiate, they seem to attach to the inner side of the epithelial 'fold', apparently connecting it to the base of the stylet and to the epithelium surrounding the ejaculatory duct and male atrium.

The common genital atrium empties into a single, terminally positioned gonopore (Figs. 6 and 8: CGA). No muscles are present around this opening. The genital atrium is a spacious, tubular cavity, 107–168 µm long ($\bar{X}$ = 145 µm, s = 28.4 µm, n = 5) and 48–62 µm wide ($\bar{X}$ = 57 µm, s = 5.7 µm, n = 5), with one outlier of 217 µm × 71 µm. It is lined by high epithelial cells (Figs. 6 and 8). Each cell displays numerous protrusions that extend into the genital atrium, giving the impression of very long cilia. Epithelial nuclei are large and round here: they have a diameter of 4–5 µm and occur just apically from the basement membrane. Uterus, male atrium, and female atrium all empty into the common genital atrium (Figs. 6 and 8).

### 3.2. Preliminary observations of reproduction in *Syndesmis kurakaikina* n. sp.

High numbers of adult endosymbionts were able to survive incubation in AFSW after removal from the gut of *E. chloroticus*. Flatworms incubated at 11.0, 14.5, and 18.0 °C had a survival rate of > 95% at the end of the four-day incubation period. Survival at higher temperatures was impaired after four days: at 21.5 °C, the

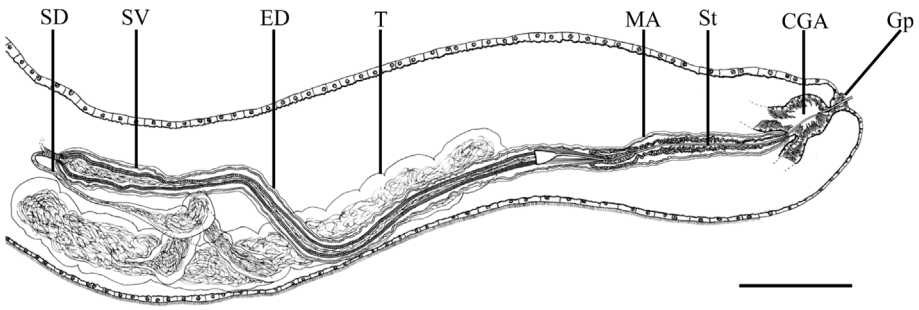


**Fig. 10.** Reconstruction of the male reproductive system from a sagittally sectioned specimen of *Syndesmis kurakaikina* n. sp. Intestine and female reproductive system omitted. Stylet not drawn in its entirety. Scale bar: 200 µm. CGA: common genital atrium, ED: ejaculatory duct, Gp: gonopore, MA: male atrium, T: testis, SD: sperm duct, St: stylet, SV: seminal vesicle.

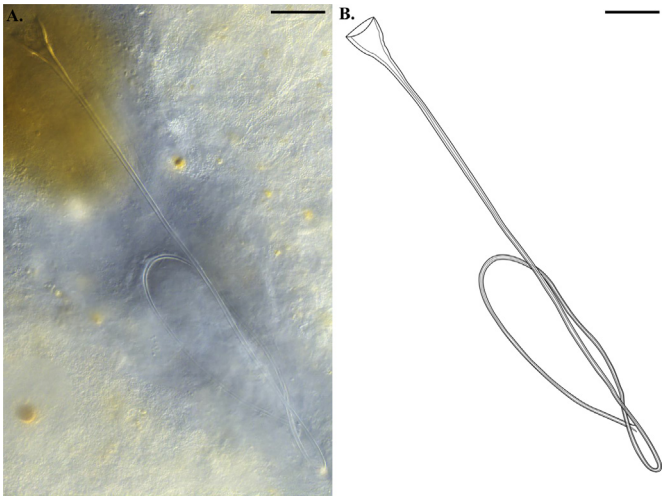


**Fig. 11.** Stylet of *Syndesmis kurakaikina* n. sp. **A.** Projection of 36 interference-contrast photographs at different focal depths. **B.** Camera-lucida drawing of this stylet. Scale bar: 50 µm.

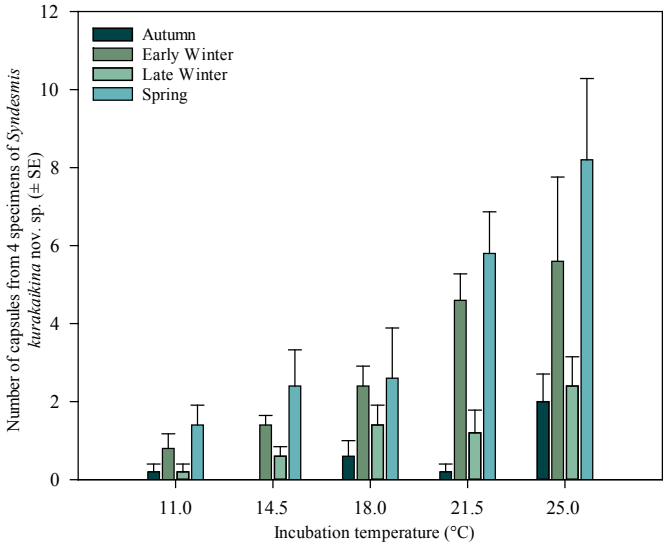


**Fig. 13.** Number of egg capsules produced by four specimens of *Syndesmis kurakaikina* n. sp., when incubated at five different temperatures (11.0, 14.5, 18.0, 21.5, and 25.0 °C). Endosymbionts were collected at four different times throughout the year (autumn, early winter, late winter and spring). 95% confidence intervals are provided.

average rate of survival reduced slightly to 92.5 ± 4.10% by Day 4; and at 25.0 °C, the average survival rate reduced to 81.3 ± 6.76% by Day 3 and 73.8 ± 8.79% by Day 4 (Mean ± SE).

Egg capsules are produced inside the uterus one at a time (Fig. 12A) and are released via the gonopore (Fig. 12B). The number of egg capsules laid in each vial (by four endosymbionts after four days incubation) differed significantly with temperature (ANOVA, $F_{(4,64)} = 22.44$, $P < 0.001$) and with season (ANOVA, $F_{(3,16)} = 7.86$, $P = 0.002$) but with a significant interaction effect between temperature and season (ANOVA, $F_{(12,64)} = 2.06$, $P = 0.032$, see below). In general, as temperature increased, so did egg-capsule production (Fig. 13), with the highest output at 25 °C in the spring experiments (mean 8.2, range 5–16 per vial). However, these patterns were complex, with both season and the urchin from which the endosymbionts were sourced affecting capsule production (Clark, 2017, unpublished Honours Dissertation). On average, capsules were produced every 24, 14, 9, 5, and 3 days at

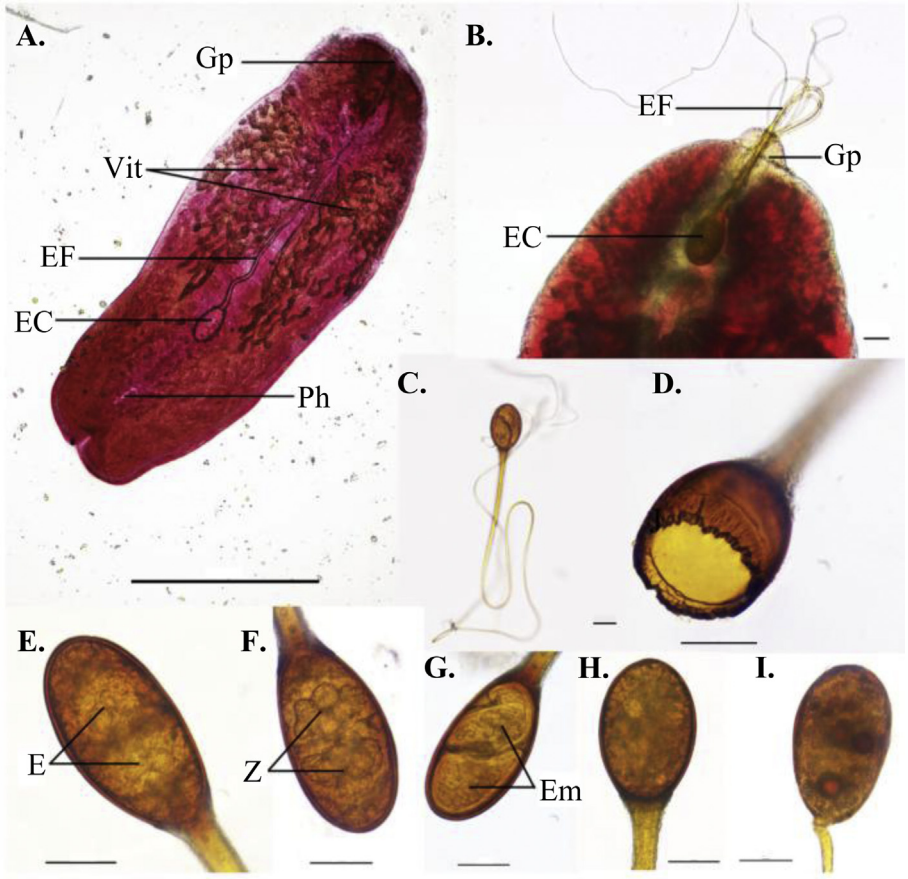


**Fig. 12.** *Syndesmis kurakaikina* n. sp. **A.** Mature specimen. **B.** Posterior end of live mature specimen in the process of laying an egg capsule. **C.** Entire egg capsule, showing the bulb containing two embryos and the long filament. **D.** Opened, empty egg capsule post-hatching after two weeks incubation at 21.5 °C. **E-G.** Photomicrographs showing the development from eggs (after one week incubation, **E**), through zygote (after two weeks incubation, **F**) to fully developed embryo (after four weeks incubation, **G**) in an egg capsule from the 14.5 °C treatment. **H–I.** Non-viable (**H**) and deformed (**I**) egg capsules from the 25 °C treatment. E: egg, EC: egg capsule, EF: egg filament, Em: embryo, Gp: gonopore, Ph: pharynx, Vit: vitellaria, Z: zygote. Scale bars: A = 1 mm, B–C = 100 µm, D-I = 50 µm.

temperatures of 11.0, 14.5, 18.0, 21.5, and 25.0 °C, respectively.

Viable capsules always contained two embryos (Fig. 12C, E-G) but it was common that egg capsules contained no viable embryos and/or had embryos in a deformed state (Fig. 12H and I). No viable capsules were seen at 25.0 °C in any of the seasons and at 11.0 and 14.5 °C, moving embryos were only seen in the early-winter experiment. With the qualification that we are testing for viability in an un-natural situation (*in vitro* in non-gut fluid), temperatures suitable for viable development appear to be restricted to 18.0 and 21.5 °C.

Hatching could be induced in egg capsules with sea urchin intestinal fluid but only in capsules produced and incubated *in vitro* at 18.0 and 21.5 °C. There was no evidence of spontaneous hatching in seawater. When embryos hatch out of the capsules, the front quarter to third of the capsule shell breaks apart along hatching sutures, which only become visible at the onset of the hatching process (Fig. 12D).

## 4. Discussion

### 4.1. Taxonomic work

#### 4.1.1. Taxonomic position

The species described here shows all character traits of Umagillidae Wahl, 1910, put forward by Wahl (1910) and Stunkard and Corliss (1951): rhabdocoels with an endosymbiotic lifestyle in an echinoderm (or sipunculid) host; lacking rhabdites, a rostrum, dermal or adhesive glands and eyes; pharynx doliiformis positioned in the first 1/3 of the body; simple unbranched intestine; well-developed brain; one gonopore, terminal; testes and ovaries paired or unpaired; vitellaria paired, large and usually branched; testes for the large part positioned behind the pharynx; seminal vesicle present; copulatory organ with or without sclerotised structures; two separate connections between the female reproductive organs and the genital atrium (ductus communis and vagina); uterus a simple protrusion of the common genital atrium.

The presence of two testes indicates that the species belongs to Umagillinae Wahl, 1910. The original diagnosis of this subfamily was also expanded by Stunkard and Corliss (1951) and now encompasses all umagillids with an oval or elongate body, a saccate or tubular intestine, paired testes, follicular and branched vitellaria, and a ductus communis that enters the common genital atrium ventral or anterior to the male atrium. *Syndesmis kurakaikina* n. sp. corresponds in all respects to this diagnosis, placing the species indisputably within Umagillinae.

Umagillinae found living inside the intestine or coelomic cavity of echinoids typically have been assigned to either *Syndesmis* or *Syndisyrinx* Lehman, 1946. Unfortunately, taxonomic literature concerning these genera has become confusing. This is due to a combination of various misidentifications and misspellings, incomplete or inadequate species descriptions, and opposing opinions on the diagnostic value of diverse morphological traits. One of the most heavily discussed issues has been the validity of *Syndisyrinx*. We concur with Marcus (1949) in considering *Syndisyrinx* a synonym of *Syndesmis*, as did Stunkard and Corliss (1951), Hyman (1960), Jondelius (1996), and Doignon and Artois (2006). As such, *Syndesmis* contains all echinoid-infecting rhabdocoels. Today, the genus encompasses 27 valid species, including the one described in this contribution, and five undescribed species, making *Syndesmis* the largest genus of Umagillidae (McRae, 1959; Westervelt and Kozloff, 1990; Doignon and Artois, 2006; Brogger and Ivanov 2010; Brusa et al., 2017). A comprehensive overview can be found in the WoRMS database (Tyler et al. 2006–2019; WoRMS Editorial Board, 2019) and a review of the genus has recently been published by Cavaleiro et al. (2018).

Unsurprisingly in view of the above, taxonomical accounts on *Syndesmis* disagree on the diagnosis of the genus, often including character traits of arguable taxonomical value; the most-debated one being the presence of a bursal valve (e.g., Lehman, 1946; Cannon, 1982; Gevaerts et al., 1995). Generally, identification of specimens as *Syndesmis* is based on an echinoid host species and the presence of a very long, often tightly coiled egg filament, a simple, funnel-like stylet, numerous filament glands in the rear end of the body, paired vitellaria, and ovaries and testes in more or less discrete pairs (e.g., Hertel and Duszynski, 1991; Brusa et al., 2017). The internal morphology of our species conforms to all of these character traits, which justifies inclusion in *Syndesmis*.

#### 4.1.2. Taxonomic remarks and comparison to other species of Syndesmis

*Syndesmis kurakaikina* n. sp. is similar in the overall organisation of its internal morphology to its congeners. It can easily be distinguished from most other species of *Syndesmis* by its particularly long, sometimes distinctly coiled stylet. All other species of *Syndesmis* possess straight (or sometimes slightly arched) stylets, making this the first species to display pronounced loops (see Fig. 11). The only known species showing a similar stylet length are *S. albida* Kozloff and Westervelt (1990) and *S. collongistyla* Marcus (1949).

*Syndesmis albida,* found in the intestine of *Echinus esculentus* Linnaeus, 1758 (Echinidae) in France and the United Kingdom (Kozloff and Westervelt, 1990) has a comparable stylet length of up to 1 mm. However, the position of the stylet is different: in *S. albida*, the stylet originates very far anteriorly, approximately at one-third of the body length. In our specimens, the stylet base is situated at approximately 2/3 to 3/4 of the body length, regardless of whether the stylet is extended or coiled inside the body. In addition, Kozloff and Westervelt (1990) mention the presence of a sclerotised 'cup' enclosing the distal part of the stylet in *S. albida*, which is absent in our specimens. Live specimens of *S. kurakaikina* n. sp. can readily be distinguished from *S. albida* by their prominent, bright-red colour, as opposed to the white to pale pink shade of the latter species. In addition, the anteriormost branches of the vitellaria are notably shorter in *S. albida*, while all branches reach approximately the same length in our specimens. Testes in *S. kurakaikina* n. sp. are very long, extending from the pharynx to approximately 2/3 of the body length and completely overlapping with the vitellaria. In *S. albida*, testes appear much more compact and only reach the anteriormost part of the vitellaria. Furthermore, testes are more or less confined to the lateral body margins in *S. albida*, which is not the case for *S. kurakaikina* n. sp. Finally, egg capsules are notably wider in *S. albida*, being 'usually 180–190 μm wide' (Kozloff and Westervelt, 1990), as opposed to an average of 122 μm in our specimens.

*Syndesmis collongistyla* is known exclusively from Caribbean waters, where it has been collected from the intestine of five different species of echinoids (Hertel and Duszynski, 1991; Doignon and Artois, 2006). It differs from *S. kurakaikina* n. sp. in the shape and position of the testes: in *S. collongistyla* these are small and globular and they are positioned rostral to the vitellaria, while in *S. kurakaikina* n. sp. the testes are more elongate and overlap completely with the vitellaria. Furthermore, the entire epidermis is ciliated in *S. collongistyla*, while in our specimens ciliation is almost entirely limited to the ventral side.

From the above it is clear that the specimens we studied belong to a new species: *Syndesmis kurakaikina* n. sp. So far, three species of *Syndesmis* have been described from Oceania: *S. cannoni* Jondelius (1996); *S. pallida* (Hickman, 1956) Marcus (1949); and *S. punicea* Hickman (1956). *Syndesmis cannoni* is known exclusively from its type host *Ammotrophus arachnoides* (Clark, 1938) Mortensen (1948) (Clypeasteridae) in Western Australia, and has not been recorded again since its original description. Likewise, *S. pallida* and *S. punicea* have not been found again since their initial recording in Tasmania. *Syndesmis pallida* has also only been retrieved from the intestine of its type host, *Echinocardium cordatum* Pennant, 1777 (Loveniidae), and *S. punicea* has been found in two different urchin species: *Heliocidaris erythrogramma* (Valenciennes, 1846) Mortensen, 1943a (Echinometridae) and *Amblypneustes ovum* (Lamarck, 1816) Mortensen, 1943b (Temnopleuridae).

As mentioned in the introduction of this study, *Syndesmis*-like flatworms have been reported from *E. chloroticus* by McRae (1959), Dix (1970), and James (2007). To our knowledge, no preserved material of these specimens exists and only a very limited characterisation of the

specimens was provided by McRae (1959). The flatworm observed by McRae (1959) does seem to share some morphological traits with *S. kurakaikina* n. sp., including a bright-red colour and a comparable body length and width. McRae's specimens seem to differ from *S. kurakaikina* n. sp. in overall body shape, as none of our specimens appears concave. Arguably, this could be attributed to differing fixation methods but no details were provided in his work. In addition, infection intensity for our species is up to two orders of magnitude higher than the two to three specimens per host McRae reported. With the data available it cannot be determined whether the specimens retrieved by these authors belong to *S. kurakaikina* n. sp.

It is also worth mentioning here that the anterior, ciliated invagination is similar to the sensory pits described for *Syndesmis selknami* Brusa et al. (2017) (although these pits are located dorsally). The food particles we observed are likely to be ciliate protozoans, which are known to occur in the intestine of *E. chloroticus* (Dix, 1970). Various ciliate species have been shown to constitute the diet of other species of *Syndesmis* (Jennings and Mettrick, 1968; Mettrick and Jennings, 1969; Holt and Mettrick, 1975). Finally, the slight expansion at the posterior end of the egg filament is similar to what has been reported for *S. aethopharynx* Westervelt and Kozloff (1990) (Monnens et al., 2017), *S. selknami*, and *S. aonikenki* Brusa et al. (2017).

#### 4.1.3. Diagnosis

Syndesmis kurakaikina *n. sp.: bright-red species of* Syndesmis*, infesting the intestine of* Evechinus chloroticus. *Ventral epidermis ciliated except over the posterior 1/10 of the body. Dorsal epidermis devoid of cilia except over the first 1/10 of the body. Stylet usually coiled inside the male canal, measuring 845 –* 1121 µm ( $\bar{X}$ = 984 µm*, s = 98.*7 µm*, n = 18*), *40–50% of the total body length. Stylet base positioned in the second body half. Paired ovaries, each with three lobes. Paired vitellaria, each with six to eight main trunks. Elongate, paired testes, extending from the hind end of the pharynx to 2/3 of the body length. Two wide sperm ducts originating from the centre of each testis, each briefly running towards the anterior before uniting with its counterpart.*

### 4.2. Reproductive characteristics

Our preliminary experiments have shown that adult *S. kurakaikina* n. sp. can be removed from the host, cultured short-term (4-days) in AFSW with high survivability, and can produce egg capsules over a wide range of temperatures (11.0–25.0 °C). Observed *in vitro* egg production rates of one capsule every 6.9 days of this species (averaged across temperatures) are comparable to those of the few other umagillids that have been studied, although in the lower part of the spectrum documented for endosymbiotic flatworms, including those with complex (cestodes and digeneans) and simple (monogeneans and turbellarians) life cycles (Whittington, 1997). A similar production rate of one capsule every 7.6 days was reported by Shinn (1983a) in *Syndesmis franciscana* (Lehman, 1946) Marcus (1949), when kept at local seawater temperatures (8–12 °C). In similar conditions, a higher production rate of approximately one capsule per day for small and nine per day for larger specimens has been observed in the sea cucumber infesting umagillid species *Anoplodium hymanae* (Shinn, 1983a, 1985).

Viable capsules of *S. kurakaikina* n. sp. consistently contained two embryos; lower than in *S. franciscana*, in which up to six embryos developed within one capsule (Shinn, 1983b), and in *A. hymanae*, which predominately contained only one zygote (Shinn, 1985). Egg capsules of *S. kurakaikina* n. sp. also differ in size and structure from those previously described: at 125 µm long and 85 µm wide (measured on live specimens), these capsules are approximately half the size of *S. franciscana* capsules and of similar size to medium sized capsules of *A. hymanae*, which vary from 75 to 250 µm in length and 45–97 µm in width (Shinn, 1983b, 1985). It is, therefore, likely that the number of embryos incorporated in capsules of umagillids is related to the capsule's size. The outer surface of capsules in the *Syndesmis kurakaikina* n. sp. is completely smooth, unlike those of previously studied species, in which surfaces are covered with lines, verrucae or ridges (Shinn, 1983b, 1985).

Development to the moving and hatching stage within the four-week study period was largely confined to capsules incubated at 18.0 and 21.5 °C, with the exception of a few capsules from the late winter and early spring that developed at cooler temperatures. Within these moderate temperatures, approximately half of all embryos reached the moving stage after one week and an average of 84% after two weeks. The majority of embryos had, therefore, reached what is probably the fully developed stage after 14 days, which is considerably sooner than the times reported for *S. franciscana* (45–50 days) or *A. hymanae* (30–35 days) at much cooler temperatures (Shinn, 1983a, 1985). Detailed analysis of development times in *S. kurakaikina* n. sp. will require improvement of the culturing methods used here to allow for individual culture of egg capsules.

In agreement with the description of the hatching process in *S. franciscana* (Shinn, 1983a) and *A. hymanae* (Shinn, 1985), hatching in *S. kurakaikina* n. sp. was induced by fluid from the anterior part of the urchin intestine only in capsules which contained live embryos at a fully developed stage. We found no evidence for spontaneous hatching in seawater as noted by Shinn (1986) in the crinoid-infecting *Fallacohospes inchoatus* Kozloff (1965) (Bicladinae, Umagillidae). The spontaneous hatching in *F. inchoatus* is thought to be an adaptation to the hosts' feeding mechanism, as dense egg capsules settle to the bottom quickly and provide limited chance for re-infection in the water column (Shinn, 1986). With *E. chloroticus* being a benthic grazer, it is, therefore, logical for infective stages of *S. kurakaikina* n. sp. to resemble those of endosymbionts of other benthic feeding echinoderms such as *S. franciscana* and *A. hymanae* and hatch in contact with the internal fluids of their host.

Temperature is an important environmental factor in determining both fecundity and developmental timing in *S. kurakaikina* n. sp. The increased *in vitro* fecundity observed with increasing temperatures is in accordance with the results of studies targeting monogenean fish parasites (Tubbs et al., 2005; Lackenby et al., 2007; Hirazawa et al., 2010; Turgut et al., 2011; Brazenor and Hutson, 2015). We do note, however, that the *in vitro* rate of capsule production reported here may differ from that of the worms in their natural environment — particularly as flatworms were deprived of feeding opportunities and therefore became progressively more starved throughout the duration of the incubation period (Whittington, 1997). Other studies, such as Shinn (1983a), found very little difference between capsule production rates *in vitro* and *in vivo* for *S. franciscana.* However, even if *in vitro* and *in vivo* rates differ in *S. kurakaikina* n. sp., the overall trend of a positive response in fecundity to higher temperatures observed here (Fig. 13) is likely a good indicator of the effect temperature will have in nature. These findings highlight the potential for increased infection risk of urchins during warmer times of the year or in years with higher overall temperatures when *S. kurakaikina* n. sp. may be able to complete an increased number of life cycles each year.

A temperature of 25.0 °C may, however, be an upper threshold for successful reproduction in *S. kurakaikina* n. sp. No viable or hatched embryos were observed at 25.0 °C and the embryos present were frequently deformed. It may be that the high rate of capsule production and release at this temperature is a stress response, with some capsules being expelled from adult flatworms prior to being fully formed. Increased reproductive effort in response to stressors that threaten an organism's survival may be adopted as a strategy to increase the final contribution of offspring to the next generation and has been observed in various species (e.g., Barry, 1989; Brannelly et al., 2016). Since a greater number of adult worms died when exposed to the 25.0 °C temperature treatment, it is possible that increased egg-capsule production was a terminal investment response by *S. kurakaikina* n. sp.

Overall, the results of this study suggest that the temperature optimum for *S. kurakaikina* n. sp. proliferation lies somewhere between

18.0 and 21.5 °C, with decreasing performance in the range of 21.5–25.0 °C. We hypothesise that an increase in future seawater temperatures due to global warming may increase the abundance and intensity of infection in sea urchin populations. Future research will need to determine the distance that egg capsules are dispersed from their source host: if there is limited dispersal, then the source urchin might re-infect itself, leading to higher endosymbiont loads; if dispersal is more extensive, there may be the potential for infection of more distant urchin populations. However, since the New Zealand sea urchin's ability to function also becomes compromised at temperatures above 21 °C (Delorme and Sewell, 2013, 2016), movement of the host away from warmer zones would probably prevent its symbionts from being exposed to temperatures beyond their optimum.

## 5. Conclusions

A new species of *Syndesmis* is formally described from the New Zealand sea urchin *Evechinus chloroticus* (Echinometridae). This species, named *S. kurakaikina* n. sp., was found infesting the intestines of *E. chloroticus* in high infection intensities. It is the fourth species of *Syndesmis* from Oceania. Among other morphological traits, *S. kurakaikina* n. sp. can easily be distinguished from its congeners by the unique combination of an unusually long (~1 mm) coiled stylet and a bright-red colour. In addition, we present an overview of the different life stages of *S. kurakaikina* n. sp. and the timing of its life cycle across a range of temperatures. *Syndesmis kurakaikina* n. sp. has moderate fecundity levels and short development times compared to other umagillids. Although variable between seasons and individuals, its *in vitro* fecundity and the timing of early development were shown to increase significantly with increasing temperature up to 21.5 °C, thus highlighting the species' increased proliferation potential in years of unusually warm seawater temperatures. Although embryonic development was compromised at 25.0 °C, *S. kurakaikina* n. sp. is unlikely to be exposed to temperatures this high, as these are above the thermal limit of the host.

## Conflict of interest

The authors have no conflict of interest to declare.

## Funding

None of the mentioned funding bodies were involved in study design; collection, analysis, and interpretation of data; writing of the report; or decision to submit this article for publication.

## Acknowledgements

M.M. is supported by a PhD fellowship of the Research Foundation Flanders (FWO-Vlaanderen). The authors are grateful to Mrs. Natascha Steffanie for sectioning and staining the specimens and to Mrs. Esther Smisdom for her assistance in preparing the focus-stacked image of the stylet. We thank Isaac Bishara (Ngāti Tūwharetoa, Ngāti Ranginui) for suggesting the species name. Part of the research leading to results presented in this publication was carried out with infrastructure funded by EMBRC Belgium -FWO project GOH3817N.

## Appendix A. Supplementary data

Supplementary data to this article can be found online at https://doi.org/10.1016/j.ijppaw.2019.07.005.

## References

Agardh, C.A., 1817. Synopsis Algarum Scandinaviæ, Adjecta Dispositione Universali Algarum. Ex officina Berlingiana, Lund, Sweden.

Agardh, J.G., 1848. Species genera et ordines algarum, seu descriptiones succinctae specierum, generum et ordinum, quibus algarum regnum constituitur. Volumen Primum. Algas fucoideas complectens. C.W.K. Gleerup, Lund, Sweden.

Altizer, S., Ostfeld, R.S., Johnson, P.T.J., Kutz, S., Harvell, C.D., 2013. Climate change and infectious diseases: from evidence to a predictive framework. Science 341, 514–519.

Barker, M.F., 2013. Chapter 24 - *Evechinus chloroticus*. In: Lawrence, J.M. (Ed.), Sea Urchins: Biology and Ecology. 38. Elsevier, Amsterdam, the Netherlands, pp. 355–368.

Barry, J.P., 1989. Reproductive response of a marine annelid to winter storms: an analog to fire adaptation in plants? Mar. Ecol. Prog. Ser. 54, 99–107.

Brannelly, L.A., Webb, R., Skerratt, L.F., Berger, L., 2016. Amphibians with infectious disease increase their reproductive effort: evidence for the terminal investment hypothesis. Open Biol. 6, 150251.

Brazenor, A.K., Hutson, K.S., 2015. Effects of temperature and salinity on the life cycle of *Neobenedenia* sp. (Monogenea: Capsalidae) infecting farmed barramundi (*Lates calcarifer*). Parasitol. Res. 114, 1875–1886.

Brogger, M.I., Ivanov, V.A., 2010. *Syndesmis patagonica* n. sp. (Rhabdocoela: Umagillidae) from the sea urchin *Arbacia dufresnii* (Echinodermata: Echinoidea) in patagonia, Argentina. Zootaxa 2442, 60–68.

Brusa, F., Montes, M.M., Marcotegui, P., Martorelli, S.R., 2017. Two new species of *Syndesmis* (Platyhelminthes, Rhabdocoela, Umagillidae) from the sea urchin *Pseudechinus magellanicus* (Echinodermata, Echinoidea) in the Southwestern Atlantic ocean. Int. J. Parasitol. Parasites Wildl 6, 54–58.

Byrne, M., Ho, M., Selvakumaraswamy, P., Nguyen, H.D., Dworjanyn, S.A., David, A.R., 2009. Temperature, but not pH, compromises sea urchin fertilization and early development under near-future climate change scenarios. Proc. R. Soc. B 276, 1883–1888.

Cannon, L.R.G., 1982. Endosymbiotic umagillids (Turbellaria) from holothurians of the great barrier reef. Zool. Scripta 11, 173–188.

Carlson, C.J., Burgio, K.R., Dougherty, E.R., Phillips, A.J., Bueno, V.M., Clements, C.F., Castaldo, G., Dallas, T.A., Cizauskas, C.A., Cumming, G.S., Doña, J., Harris, N.C., Jovani, R., Mironov, S., Muellerklein, O.C., Proctor, H.C., Wayne, M.G., 2017. Parasite biodiversity faces extinction and redistribution in a changing climate. Sci. Adv. 3, e1602422.

Cavaleiro, F.I., Frade, D.G., Rangel, L.F., Santos, M.J., 2018. *Syndesmis* François, 1886 (Rhabdocoela: Umagillidae): a revisitation, with a synopsis and an identification key to species, and new molecular evidence for ascertaining the phylogeny of the group. Syst. Parasitol. 95, 147–171.

Clark, D., Lamare, M., Barker, M., 2009. Response of sea urchin pluteus larvae (Echinodermata: Echinoidea) to reduced seawater pH: a comparison among a tropical, temperate, and a polar species. Mar. Biol. 156, 1125–1137.

Clark, H.L., 1938. Echinoderms from Australia, an Account of Collections Made in 1929 and 1932. Memoirs of the Museum of Comparative Zoology at Harvard College v.55, Cambridge, Massachusetts, United States.

Clark, M., 2017. The Effect of Temperature on the Metabolism, Biochemistry and Early Life Stages of the Parasitic Flatworm *Syndesmis* N. Sp. Inhabiting the Intestine of the new zealand Sea Urchin, *Evechinus chloroticus*. Bachelor of Science (Honours). University of Auckland.

Delorme, N.J., Sewell, M.A., 2013. Temperature limits to early development of the New Zealand sea urchin *Evechinus chloroticus* (Valenciennes, 1846). J. Therm. Biol. 38, 218–224.

Delorme, N.J., Sewell, M.A., 2016. Effects of warm acclimation on physiology and gonad development in the sea urchin *Evechinus chloroticus*. Comp. Biochem. Physiol. Mol. Integr. Physiol. 198, 33–40.

Dix, T.G., 1970. Biology of *Evechinus chloroticus* (Echinoidea: Echinometridae) from different localities. N. Z. J. Mar. Freshw. Res. 4, 91–116.

Doignon, G., Artois, T., 2006. Annotated checklist of the umagillid turbellarians infesting echinoids (Echinodermata). Belg. J. Zool. 136, 101–106.

Dupont, S., Ortega-Marínez, O., Thorndyke, M., 2010. Impact of near-future ocean acidification on echinoderms. Ecotoxicology 19, 449–462.

Gevaerts, H., Moens, J.B., Martens, E.E., Schockaert, E.R., 1995. Hard parts in the female system of *Syndesmis longicanalis* (Platyhelminthes, Rhabdocoela, Umagillidae) are basement membrane derivatives. Invertebr. Biol. 114, 279–284.

Hertel, L.A., Duszynski, D.W., 1991. *Syndisyrinx evelinae* (Marcus, 1968) n. comb., from the rock-boring urchin, *Echinometra lucunter*, from St. Barthélemy. J. Parasitol. 77, 638–639.

Hertel, L.A., Duszynski, D.W., Ubelaker, J.E., 1990. Turbellarians (Umagillidae) from Caribbean urchins with a description of *Syndisyrinx collongistyla* n. sp. Trans. Am. Microsc. Soc. 109, 273–281.

Hickman, V.V., 1956. Parasitic Turbellaria from tasmanian echinoidea. Pap. Proc. R. Soc. Tasman. 90, 169–181.

Hirazawa, N., Takano, R., Hagiwara, H., Noguchi, M., Narita, M., 2010. The influence of different water temperatures on *Neobenedenia girellae* (Monogenea) infection, parasite growth, egg production and emerging second generation on amberjack *Seriola dumerili* (Carangidae) and the histopathological effect of this parasite on fish skin. Aquaculture 299, 2–7.

Holt, P.A., Mettrick, D.F., 1975. Ultrastructural studies of the epidermis and gastrodermis of *Syndesmis franciscana* (Turbellaria: Rhabdocoela). Can. J. Zool. 53, 536–549.

Hyman, L.H., 1960. New and known umagillid rhabdocoels from echinoderms. Am. Mus. Novit. 1–14 1984.

International Commission on Zoological Nomenclature, 2015. Chapter 11: Authorship. Article 50: Authors of Names and Nomenclatural Acts. International Code of Zoological Nomenclature, fourth ed. .

IPCC, 2014. In: Pachauri, R.K., Meyer, L.A. (Eds.), Climate Change 2014: Synthesis Report. Contribution of Working Groups I, II and III to the Fifth Assessment Report of the Intergovernmental Panel on Climate Change [The Core Writing Team, (Geneva,

Switzerland).
James, P., 2007. The Effects of Environmental Factors and Husbandry Techniques on Roe Enhancement of the New Zealand Sea Urchin, *Evechinus chloroticus*. PhD Thesis. Victoria University of Wellington.
Jennings, J.B., Mettrick, D.F., 1968. Observations on the ecology, morphology and nutrition of the rhabdocoel turbellarian *Syndesmis franciscana* (Lehman, 1946) in Jamaica. Caribb. J. Sci. 8, 57–69.
Jondelius, U., 1996. Three echinoderm inhabiting flatworms (Platyhelminthes, Rhabdocoela) from Western Australia. Belg. J. Zool. 126, 37–48.
Kozloff, E.N., 1965. *Desmote inops* sp. n. and *Fallacohospes inchoatus* gen. and sp. n., umagillid rhabdocoels from the intestine of the crinoid *Florometra serratissima* (A. H. Clark). J. Parasitol. 51, 305–312.
Kozloff, E.N., Westervelt, C.A.J., 1990. *Syndesmis rubida* sp. nov. and *S. albida* sp. nov. (Turbellaria: Neorhabdocoela: Umagillidae) from the sea urchin *Echinus esculentus*. Cah. Biol. Mar. 31, 323–332.
Lackenby, J.A., Chambers, C.B., Ernst, I., Whittington, I.D., 2007. Effect of water temperature on reproductive development of *Benedenia seriolae* (Monogenea: Capsalidae) from *Seriola lalandi* in Australia. Dis. Aquat. Org. 74, 235–242.
Lamarck, J.-B.M., 1816. Histoire naturelle des animaux sans vertèbres. Tome troisième. Deterville/Verdière, Paris, France.
Lehman, H., 1946. A histological study of *Syndisyrinx franciscanus*, gen. et sp. nov., an endoparasitic rhabdocoel of the sea urchin, *Strongylocentrotus franciscanus*. Biol. Bull. 91, 295–311.
Linnaeus, C., 1758. Systema Naturæ Per Regna Tria Naturæ, Secundum Classes, Ordines, Genera, Species, Cum Characteribus, Differentiis, Synonymis, Locis. Laurentius Salvius, Stockholm, Sweden.
Macnab, V., Barber, I., 2011. Some (worms) like it hot: fish parasites grow faster in warmer water, and alter host thermal preferences. Glob. Chang. Biol. 18, 1540–1548.
Marcogliese, D.J., 2001. Implications of climate change for parasitism of animals in the aquatic environment. Can. J. Zool. 79, 1331–1352.
Marcus, E., 1949. Turbellaria brasileiros (7). Bol. Fac. Fil. Ciênc. Letr. Univ. São Paulo, zool. 14, 7–155.
McRae, A., 1959. *Evechinus chloroticus* (Val.), an endemic New Zealand echinoid. T. Roy. Soc. N. Z. 86, 204–267.
Mettrick, D.F., Jennings, J.B., 1969. Nutrition and chemical composition of the rhabdocoel turbellarian *Syndesmis franciscana*, with notes on the taxonomy of *S. antillarum*. J. Fish. Res. Board Can. 26, 2669–2679.
Miller, S.L., Abraham, E.R., 2011. Characterisation of New Zealand Kina Fisheries. New Zealand Fisheries Assessment Report 2011/7. Ministry of Fisheries, Wellington, New Zealand.
Minot, C.S., 1876. Studien an Turbellarien. Beitrage zur Kenntnis der plathelminthen. Arb Zool-Zoot Inst Wurzburg, III. Bd. Hamburg 405–471 Fig 16-20.
Moens, J.B., Martens, E.E., Schockaert, E.R., 1994. *Syndesmis longicanalis* sp. nov., an umagillid turbellarian (Plathelminthes) from echinoids from the Kenyan coast. Belg. J. Zool. 124, 105–114.
Monnens, M., Artois, T., Vanhove, M.P.M., 2017. *Syndesmis aethopharynx* (Umagillidae, Rhabdocoela, Platyhelminthes) from the sea urchin *Paracentrotus lividus*: first record from the Eastern Mediterranean, phylogenetic position and intraspecific morphological variation. Parasitol. Int. 66, 848–858.
Mortensen, T., 1943a. A Monograph of the Echinoidea. III. 3. Camarodonta. II. Echinidæ, Strongylocentrotidæ, Parasaleniidæ. Echinometridæ. C.A. Reitzel, Copenhagen, Denmark.
Mortensen, T., 1943b. A Monograph of the Echinoidea. III, 2. Camarodonta. I. Orthopsidæ, Glyphocyphidæ, Temnopleuridæ and Toxopneustidæ. C.A. Reitzel, Copenhagen, Denmark.
Mortensen, T., 1948. A Monograph of the Echionidea. IV, 2. Clypeasteroida. Clypeasteridæ, Arachnoidæ, Fibulariidæ, Laganidæ and Scutellidæ. C. A. Reitzel, Copenhagen, Denmark.
Pennant, T., 1777. British Zoology: IV. Crustacea. Mollusca. Testacea: I-Viii. William Eyres, Warrington, United Kingdom.
Poulin, R., 2005. Global warming and temperature-mediated increases in cercarial emergence in trematode parasites. Parasitology 132, 143–151.
Przeslawski, R., Byrne, M., Mellin, C., 2015. A review and meta-analysis of the effects of multiple abiotic stressors on marine embryos and larvae. Glob. Chang. Biol. 21, 2122–2140.
R Development Core Team, 2017. R: a Language and Environment for Statistical Computing. R Foundation for Statistical Computing, Vienna, Austria Available from: http://www.R-project.org/.
Shears, N.T., Bowen, M.M., 2017. Half a century of coastal temperature records reveal complex warming trends in western boundary currents. Sci. Rep. 7, 14527.
Shinn, G.L., 1983a. The life history of *Syndisyrinx franciscanus*, a symbiotic turbellarian from the intestine of echinoids, with observations on the mechanism of hatching. Ophelia 22, 57–79.
Shinn, G.L., 1983b. *Anoplodium hymanae* sp. n., an umagillid turbellarian from the coelom of *Stichopus californicus*, a Northeast Pacific holothurian. Can. J. Zool. 61, 750–760.
Shinn, G.L., 1985. Reproduction of *Anoplodium hymanae*, a turbellarian flatworm (Neorhabdocoela, Umagillidae) inhabiting the coelom of sea cucumbers; production of egg capsules, and escape of infective stages without evisceration of the host. Biol. Bull. 169, 182–198.
Shinn, G.L., 1986. Spontaneous hatching of *Fallacohospes inchoatus*, un umagillid flatworm from the northeastern Pacific crinoid *Florometra serratissima*. Can. J. Zool. 64, 2068–2071.
Silliman, W., 1881. Sur un nouveau type de Turbellariés. C. R. Hebd. Seances Acad. Sci. 93, 1087–1089.
Smith, N.S., 1973. A new description of *Syndesmis dendrastrorum* (Platyhelminthes, Turbellaria), an intestinal rhabdocoel inhabiting the sand dollar *Dendraster excentricus*. Biol. Bull. 145, 598–606.
Stunkard, H.W., Corliss, J.O., 1951. New species of *Syndesmis* and a revision of the family Umagillidae Wahl, 1910 (Turbellaria: Rhabdocoela). Biol. Bull. 101, 319–334.
Tubbs, L.A., Poortenaar, C.W., Sewell, M.A., Diggles, B.K., 2005. Effects of temperature on fecundity in vitro, egg hatching and reproductive development of *Benedenia seriolae* and *Zeuxapta seriolae* (Monogenea) parasitic on yellowtail kingfish *Seriola lalandi*. Int. J. Parasitol. 35, 315–327.
Turgut, E., Ozgul, G., Buhan, E., 2011. Seasonal changes of metazoan parasites in *Capoeta tinca* and *Capoeta capoeta* in Almus dam lake, Turkey. Bull. Eur. Assoc. Fish Pathol. 31, 23–30.
Tyler, S., Artois, T., Schilling, S., Hooge, M., Bush, L.F. (Eds.), 2006-2019. World List of Turbellarian Worms: Acoelomorpha, Catenulida, Rhabditophora. *Syndesmis* Silliman, 1881, Retrieved 2019-06- 27, Available from: World Register of Marine Species at: http://www.marinespecies.org/aphia.php?p=taxdetails&id=142304.
Valenciennes, A., 1846. Zoophytes. In: Du Petit Thouars, A.-A. (Ed.), Voyage autour de monde sur la frégate La Vénus, pendant les années 1836-1839. Atlas de Zoologie Gide et Cie, Paris, France.
Villouta, E., Chadderton, W.L., Pugsley, C.W., Hay, C.H., 2001. Effects of sea urchin (*Evechinus chloroticus*) grazing in dusky sound, Fiordland, New Zealand. N. Z. J. Mar. Freshw. Res. 35, 1007–1023.
Wahl, B., 1910. Beitrage zur Kenntnis der Dalyelliiden und Umagilliden. Fetschrift zum sechzigsten Geburstag Richard Hertwigs (München). Gustav Fischer, Jena, Germany, pp. 41–60 + 2 Pl.
Westervelt, C.A.J., Kozloff, E.N., 1990. *Syndesmis aethopharynx* sp. nov. (Turbellaria: Neorhabdocoela: Umagillidae), from the sea urchin *Paracentrotus lividus*, with notes on a probable third species from this host. Cah. Biol. Mar. 31, 431–437.
Whittington, I.D., 1997. Reproduction and host-location among the parasitic platyhelminthes. Int. J. Parasitol. 27, 705–714.
Wood, H.L., Spicer, J.I., Widdicombe, S., 2008. Ocean acidification may increase calcification rates, but at a cost. Proc. R. Soc. B 275, 1767–1773.
WoRMS Editorial Board, 2019. World register of marine species. Available from. http://www.marinespecies.org.